

Magnetic properties of terbium in the paraprocess region

B. K. Ponomarev and N. I. Moreva

Institute of Solid State Physics, USSR Academy of Sciences

(Submitted May 5, 1975)

Zh. Eksp. Teor. Fiz. 69, 1352-1361 (October 1975)

We measured the magnetization of single-crystal terbium in the easy-magnetization direction (basal plane of the crystal) in a pulsed magnetic field of intensity up to 380 kOe and duration 0.01 sec, and in the interval 80-380°K. It is shown that the equal-magnetization lines of terbium differ qualitatively from the equal-magnetization lines of the alloys $\text{Fe}_{65}(\text{Ni}_{1-x}\text{Mn}_x)_{35}$ in a wide range of fields and temperatures. This is attributed to the difference between the types of the statistical distributions that describe the carriers of the magnetic moment in the indicated substances. It is proposed that the observed difference in the behavior of the equal-magnetization lines exists not only between terbium and iron-nickel-manganese alloys, but also between ferromagnetic-metal groups 4f and 3d. It is shown that from the equal-magnetization lines of terbium it is possible to determine the molecular field as a function of the magnetization. The molecular field of terbium at magnetization values on the order of $300 \text{ G}\cdot\text{cm}^3/\text{g}$ reaches 900 kOe.

PACS numbers: 75.50.Cc

In spite of the intensive investigations of the magnetic properties of rare-earth metals, there are not enough published detailed experimental data on the dependence of their magnetization on the field and temperature at large field values, where the field dependence of the magnetization is determined by the change of the magnetic-order parameter (the paraprocess region). The change of the magnetization of a ferromagnet in the paraprocess region is directly connected with the exchange interaction, and an investigation of the field and temperature dependences of the magnetization in the region of the paraprocess yields information on the magnitude of the exchange interaction and on the mechanism whereby ferromagnetic order sets in.

The magnetization of terbium in fields that are strong enough for the observation of the paraprocess was investigated by a number of workers, but the measurements were performed by them only near liquid nitrogen or helium temperatures. The magnetization of terbium in a wide temperature interval was investigated in^[5], but the fields used there (up to 18 kOe) were not high enough to be able to measure reliably the change of the magnetization as a result of the paraprocess in the ferromagnetic region.

In connection with the foregoing, it is expedient to measure the magnetization of terbium in a wide temperature interval in fields on the order of 300-400 kOe. We have measured the magnetization of a single-crystal sample of terbium in the basal plane, which is the easy-magnetization plane. We investigated a terbium sample in the form of a rectangular parallelepiped 10 mm long and 1×1 mm in cross section. The long side of the sample coincided with the basal plane of the crystal. The deviation from the basal plane, according to x-ray data, did not exceed 1° . The orientation in the basal plane was arbitrary. The measurements were performed by an induction method^[6] in a pulsed magnetic field of intensity up to 380 kOe and duration 0.01 sec, in the temperature interval from 80 to 300°K .

The temperature interval in which a canted antiferromagnetic structure exists in terbium is relatively small, from 219 to 230°K ,^[7] and the magnetic field that destroys the antiferromagnetism does not exceed 0.2 kOe. There was therefore no antiferromagnetism in practically the entire field and temperature interval investigated by us.

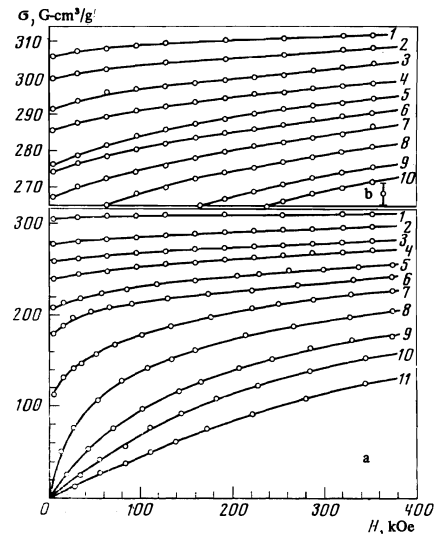


FIG. 1. Magnetization adiabats of terbium single crystal in the basal plane for different initial sample temperatures T_0 : a) curve 1-80, 2-130, 3-155, 4-174.5, 5-194.5, 6-210.5, 7-224.5, 8-250.5, 9-293, 10-321, 11-372 K; b) curve 1-80, 2-91, 3-108, 4-119.5, 5-133.5, 6-138, 7-148, 8-155, 9-168.5, 10-174.5 K.

Figure 1 shows some of the obtained magnetization adiabats of terbium at different values of the initial sample temperature T_0 . Adiabats 8-11 on Fig. 1 describe the behavior of the magnetization of terbium in the paramagnetic region (the temperature of the magnetic ordering of terbium is $\Theta = 230^\circ\text{K}$ ^[7]). The remaining curves in Figs. 1a and 1b were measured in the ferromagnetic region. Figure 1b shows the magnetization adiabats measured close to liquid-nitrogen temperature. The magnetization scale on Fig. 1b is four times larger than in Fig. 1a.

The increase of the magnetization with increasing field is due to the paraprocess in almost the entire field interval. The influence of the sixth-order magnetocrystal anisotropy in the basal plane can be neglected, since the effective field of this anisotropy does not exceed 10 kOe at liquid-nitrogen temperature and decreases rapidly with rising temperature.

The curves of Figs. 1a and 1b thus describe the magnetization of a one-domain sample with a magnetization vector parallel to the external field. It is seen that

an increase of the field from zero to 380 kOe leads to a noticeable increase of the magnetization as a result of the paraprocess up to 90°K. In the paramagnetic region at $T = 250.5^\circ\text{K}$, i.e., 20°K above the magnetic-ordering temperature (curve 8 on Fig. 1a), an external magnetic field of intensity 380 kOe produces a magnetization exceeding $200 \text{ G}\cdot\text{cm}^3/\text{g}$, equal in magnitude to the spontaneous magnetization at 194.5°K (curve 5 on Fig. 1a), i.e., more than 30°K below the magnetic-ordering temperature. Thus, the influence of the external magnetic field on the degree of the ferromagnetic order is comparable in this case with the exchange-interaction effect.

The experimental adiabatic-magnetization lines, after taking the magnetocaloric effect into account, were used to plot the equal-magnetization lines of terbium in the (T, H) plane at different values of the magnetization. The change of the sample temperature as a result of the magnetocaloric effect was $\Delta T = T - T_0$, where T_0 is the temperature prior to turning on the pulsed magnetic field, while T , the real temperature of the sample during the adiabatic-magnetization process, amounts to 7°K at $T_0 = 80^\circ\text{K}$ and 60°K at $T_0 = 230^\circ\text{K}$ in a field of 380 kOe. In the calculation of the magnetocaloric effect it was assumed that the heat capacity of terbium C_σ at constant magnetization is constant in the investigated temperature interval and is equal to the high-temperature value $C_\sigma(T > \Theta_D) = 7 \text{ cal/mole}\cdot\text{deg}$.^[8] The Debye temperature for terbium is $\Theta_D = 144^\circ\text{K}$.^[9]

The temperature dependence of the heat capacity $C_\sigma(T)$ of terbium was investigated in^[9]. Allowance for this dependence introduces a correction $\sim(2-4)^\circ\text{K}$ to the values of the magnetocaloric effect. The corresponding correction to the slopes and the initial ordinates of the equal-magnetization lines does not exceed 4%. Figure 2 shows some of the obtained equal-magnetization lines. It is seen that, within the limits of errors, they are straight lines in the entire investigated field and temperature interval and can be described by the relation

$$H_\sigma(T) = b(\sigma)T - H_m(\sigma). \quad (1)$$

Here $H_\sigma(T)$ is the temperature dependence of the field at a specified fixed value of the magnetization σ , while $b(\sigma)$ and $-H_m(\sigma)$ are the slope and the initial ordinate of the equal-magnetization line.

The fact that the experimental equal-magnetization lines are straight means that the temperature and field dependences of the magnetization of terbium are described by the relation

$$\frac{\sigma(H, T)}{\sigma_0} = f\left[a \frac{H + H_m(\sigma)}{T}\right] = f(x). \quad (2)$$

Here $\sigma(H, T)$ is the magnetization at given values of the field H and temperature T , σ_0 is the magnetization at $H = 0$ and $T = 0^\circ\text{K}$, $f(x)$ is a certain unknown function, and a is a constant. An important factor in relation (2) is that the argument of the function $f(x)$ constitutes, apart from the constant factor a , the ratio of the sum of the external field H and a certain value $H_m(\sigma)$ to the temperature T . If we put $\sigma(H, T) = \sigma = \text{const}$ in (2), then we obtain from (2) Eq. (1), with

$$b(\sigma) = \left(\frac{\partial H}{\partial T}\right)_\sigma = \frac{1}{a} f^{-1}\left(\frac{\sigma}{\sigma_0}\right), \quad (3)$$

where $f^{-1}(\sigma/\sigma_0)$ is the reciprocal of $f(x)$. The function $f(x)$ can be obtained from the experimental dependence of the slopes $b(\sigma)$ on the magnetization with the aid of relation (3), if the values of σ_0 and a are known.

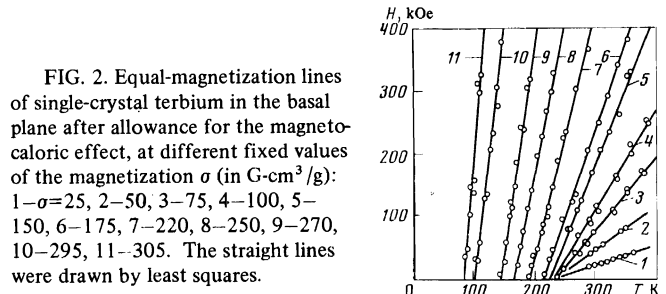


FIG. 2. Equal-magnetization lines of single-crystal terbium in the basal plane after allowance for the magnetocaloric effect, at different fixed values of the magnetization σ (in $\text{G}\cdot\text{cm}^3/\text{g}$): 1— $\sigma=25$, 2—50, 3—75, 4—100, 5—150, 6—175, 7—220, 8—250, 9—270, 10—295, 11—305. The straight lines were drawn by least squares.

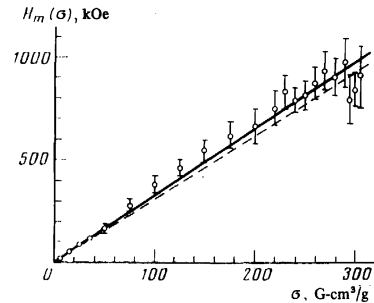


FIG. 3. Dependence of the modulus of the initial ordinate of the equal-magnetization lines of terbium on the magnetization. Straight lines—theoretical plots of the molecular field of terbium against the magnetization. Solid line— $\gamma=3.22 \times 10^3 \text{ Gm/cm}^3$, dashed line— $\gamma=3.10 \times 10^3 \text{ g/cm}^3$.

The functions $b(\sigma)$ and $H_m(\sigma)$ were obtained by a linear least-squares fit of the experimental equal-magnetization lines $H_\sigma(T)$ (Fig. 2) to relation (1) for various fixed values of the magnetization σ . Figure 3 shows the dependence of the modulus of the initial ordinate $H_m(\sigma)$ on the magnetization. It is seen that this relation is monotonic within the limits of the experimental error.

It is of interest to compare the behavior of the equal-magnetization lines of terbium and of the iron-nickel-manganese alloy system $\text{Fe}_{65}(\text{Ni}_{1-x}\text{Mn}_x)_{35}$. It was shown experimentally in^[10] that the equal-magnetization lines of these alloys in the (T, H) plane are parabolas whose initial ordinates depend on the magnetization in non-monotonic fashion and reverse sign at $\sigma = \sigma_0$.

It was thus established experimentally that there are distinct qualitative differences in the behaviors of the magnetic properties of terbium and iron-nickel-manganese alloys, as revealed by the following attributes:

1. The shapes of the equal-magnetization lines in the (T, H) plane: a) straight line in the case of terbium, b) a parabola in the case of the iron-nickel-manganese alloy.

2. The dependence of the initial ordinate of the equal-magnetization line on the magnetization: a) monotonic for terbium, nonmonotonic with sign reversal for the iron-nickel-manganese alloys.

The foregoing experimental facts can be explained in the molecular-field approximation as being due to the fact that the carriers of the magnetic moment in 4f and 3d metals are described by different statistical distributions. At the present time, the universally accepted point of view is that in rare-earth ferromagnets the magnetic moments are localized in the crystal-lattice sites, since the magnetoactive 4f electrons are screened against any external action by the 5s and 5p elec-

trons.^[7,11] Owing to the strong coupling between the magnetoactive 4f electrons and the lattice sites, the ensemble of the magnetic moments in rare-earth ferromagnets is described with good accuracy by a statistical Maxwell-Boltzmann distribution. In this case the molecular-field approximation yields for the field and temperature dependences of the magnetization the expression

$$\frac{\sigma(H, T)}{\sigma_0} = B_J \left\{ \frac{\mu_S [H + H_m(\sigma)]}{kT} \right\} = B_J(x), \quad (4)$$

$$H_m(\sigma) = \gamma\sigma. \quad (5)$$

Here k is the Boltzmann constant, B_J is the Brillouin function, J is the total quantum number, $\mu_S = gJ\mu_B$ is the maximum projection of the magnetic moment of the ion on the quantization axis, μ_B is the Bohr magneton, $H_m(\sigma)$ is the molecular field, and γ is the molecular-field constant per unit mass.

If we put $\sigma(H, T) = \text{const}$ in (4), then (4) leads to (1), with

$$b(\sigma) = \left(\frac{\partial H}{\partial T} \right)_\sigma = \frac{k}{\mu_S} B_J^{-1} \left(\frac{\sigma}{\sigma_0} \right), \quad (6)$$

where $B_J^{-1}(\sigma/\sigma_0)$ is the reciprocal of the Brillouin function. Thus, the linear character of the equal magnetization lines and the monotonic dependence of their initial ordinate on the magnetization, which were observed by us experimentally on terbium, follow from the molecular-field theory for a ferromagnet in which the magnetic-moment carriers are described by a Maxwell-Boltzmann distribution. The modulus of the initial ordinate of the equal-magnetization lines has in this case the physical meaning of the molecular field, and the constant a in relations (2) and (3) is equal to $a = \mu_S/k$.

It follows therefore that the construction of the equal-magnetization lines in the region of the paraprocess can be used as a method of experimentally determining the molecular field in ferromagnets of the indicated type. It is seen from Fig. 3 that the molecular field of terbium at large values of the magnetization reaches 900 kOe. In ferromagnets of the iron group, the magnetoactive 3d electrons on the periphery are subject to a strong action of the crystal-line environment, and are much more weakly coupled to the lattice sites than the 4f electrons in rare-earth ferromagnets. The magnetic properties of ferromagnets of the iron group can therefore, generally speaking, be subject to the effect of formation of energy bands by the 3d electrons. The statistical properties of such an ensemble of magnetic moments must be described by a Fermi-Dirac distribution. In^[12,13], in the molecular field approximation, they considered the behavior of a band ferromagnet in the limiting case when the exchange interaction is weak in comparison with the width of the energy band made up by the magnetic-moment carriers, meaning the case of very weak collectivized ferromagnetism. It was shown that for a very weak collectivized ferromagnet, in the molecular field approximation, the temperature and field dependences of the magnetization are described by the relation

$$\left[\frac{\sigma(H, T)}{\sigma_0} \right]^3 = \frac{\sigma(H, T)}{\sigma_0} \left[1 - \left(\frac{T}{T_c} \right)^2 \right] = \frac{2\chi_0 H}{\sigma_0}. \quad (7)$$

It follows therefore that the equal-magnetization lines in the (H, T) plane are parabolas whose initial ordinate depends on the magnetization nonmonotonically. At

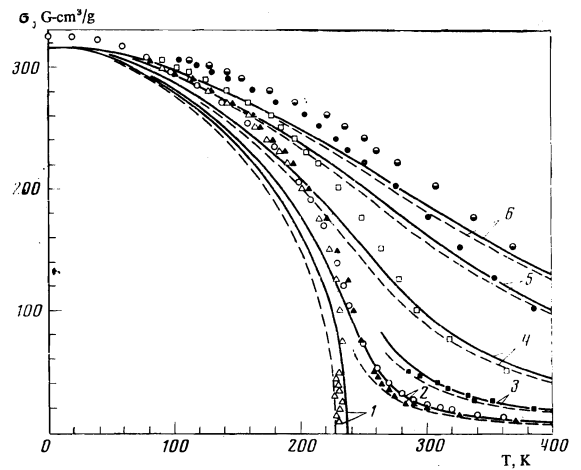


FIG. 4. Temperature dependences of the magnetization of single-crystal terbium in the basal plane at different values of the field H : Δ) 0, \blacktriangle) 18 kOe, \blacksquare) 40 kOe, \square) 100 kOe, \bullet) 250 kOe, \ominus) 1350 kOe. The values of the magnetization at $H=0$ were obtained from the intercepts of the equal-magnetization lines with the temperature axis. \circ) experimental data from^[5], $H=18$ kOe. The curves were calculated with the aid of relations (4), (5), and (8): 1) $H=0$; 2) $H=18$ kOe; 3) $H=40$ kOe; 4) $H=100$ kOe; 5) $H=250$ kOe; 6) $H=350$ kOe. Solid curves— $\ominus=Θ_p=239$ K, $\gamma=3.22 \times 10^3$ g/cm³; dashed— $\ominus=Θ_c=230$ K, $\gamma=3.10 \times 10^3$ g/cm³.

$\sigma = \sigma_0/3^{1/2}$ there is an extremum, and at $\sigma = \sigma_0$ the sign of the initial ordinate is reversed.

The behavior of the equal-magnetization lines of iron-nickel-manganese alloys, experimentally investigated in^[10], agrees well with the conclusions of the theory of very weak collectivized ferromagnetism.^[12,13]

Taking all the foregoing into account, it can be stated that the difference in the behavior of the magnetic properties of terbium and the iron-nickel-manganese alloys is due to the fact that in terbium the carriers of the magnetic moment in the investigated temperature interval are described by a Maxwell-Boltzmann distribution, as against a Fermi-Dirac distribution for the iron-nickel-manganese alloys. It can also be assumed that the indicated difference exists not only between terbium and the iron-nickel-manganese alloys, but also between the groups of the rare-earth ferromagnets and 3d ferromagnets.

Figure 4 shows the experimental temperature dependences of the magnetization of terbium in the basal plane for different fixed values of the field, obtained in the present study after taking the magnetocaloric effect into account. The values of the spontaneous magnetization were determined from the intercepts of the equal-magnetization lines with the temperature axis. For comparison, we show the experimental temperature dependence of the magnetization of terbium as measured in^[5] along the b axis in the basal plane in an 18-kOe field (light circles). It is seen that our results for $H = 18$ kOe (dark triangles) agree well with the results of^[5]. The spontaneous magnetization in Fig. 4 vanishes at $T_c = 230 \pm 4^\circ$ K. This value of the temperature differs from $\Theta_1 = 219^\circ$ K, at which the spontaneous magnetization of terbium in a zero external field vanishes, owing to the ferromagnetism-antiferromagnetism transition. The reason for the difference is that the values of the spontaneous magnetization $\sigma_S(T)$ (Fig. 4) were obtained by extrapolating the equal-magnetization lines until they

cross the temperature axis from the region of fields that exceed the critical antiferromagnetism-destruction field in terbium $H_c \leq 0.2$ kOe.^[7] The temperature $T_c = 230 \pm 4^\circ$ K should be regarded as the ferromagnetic Curie point of terbium, which is not realized, however, since in the absence of a magnetic field the antiferromagnetic structure in terbium turns out to be more stable than the ferromagnetic one in the temperature interval $\Theta_1 = 219^\circ$ K $< T < \Theta_2 = 230^\circ$ K.

The curves in Fig. 4 were calculated with the aid of relations (4) and (5) of molecular field theory. In the calculation we used the quantities $\mu_S = gJ\mu_B = 9\mu_B$ and $\sigma_0 = n\mu_S = 316$ G-cm³/g. The values $g = 3/2$ and $J = 6$ were taken for the free trivalent terbium ion,^[7,11] and $n = 3.79 \times 10^{21}$ g⁻¹ is the number of atoms per gram of terbium. The molecular-field constant γ was obtained from the relation

$$\gamma = 3k\Theta/n g^2 \mu_B^2 J(J+1). \quad (8)$$

In the molecular field theory, the quantity Θ is simultaneously the temperature at which magnetic order vanishes and the point where the linear plot of the reciprocal susceptibility against temperature, $1/\chi(T)$, crosses the temperature axis. In a real ferromagnet the vanishing of the magnetic order takes place at a temperature T_c (ferromagnetic Curie point), and lower than the temperature Θ_p (paramagnetic Curie point) at which the straight line $1/\chi(T)$ crosses the temperature axis. The calculation was therefore performed for two values of the molecular-field constant γ . The solid curves were calculated for $\gamma = 3.22 \times 10^3$ g/cm³, which corresponds to $\Theta = \Theta_p = 239^\circ$ K. The dashed curves were obtained at $\gamma = 3.10 \times 10^3$ g/cm³ and $\Theta = T_c = 230^\circ$ K. It is seen that in both cases the calculated plots deviate noticeably from the experimental ones. The smallest discrepancy between theory and experiment is observed at low values of the magnetization (curves 2 and 3).

In connection with the foregoing, it is advantageous to compare the experimental functions $H_m(\sigma)$ and $f(x)$, which enter in relation (2), with the corresponding theoretical relations (5) and (4). The theoretical $H_m(\sigma)$ are shown in Fig. 3. They were obtained from (5) for the values $\gamma = 3.22 \times 10^3$ g/cm³ (solid line) and $\gamma = 3.10 \times 10^3$ g/cm³ (dashed). At low magnetization values, the experimental $H_m(\sigma)$ agree equally well, within the limits of experimental error, with both theoretical curves, so that it is impossible to give preference to any of the obtained values of the molecular field constant γ . At large magnetizations, a systematic deviation of the experimental values of $H_m(\sigma)$ from the two theoretical lines is observed.

The experimental function $f(x)$ from relation (2) is shown in Fig. 5. It was obtained from the experimental $b(\sigma)$ with the aid of relation (3), where $a = \mu_S/k$. We used the same values of μ_S and σ_0 as for the calculation of the theoretical plots of the magnetization on Fig. 4. The solid curve shows the Brillouin function $B_J(x)$ for $J = 6$. At low values of x , good agreement is observed between theory and experiment, and at large values of x the experimental points lie systematically above the Brillouin curve. Thus, the experimental $H_m(\sigma)$ and $f(x)$ from relation (2) agree best, just as the experimental temperature dependence of the magnetization, with the molecular-field theory at low values of the magnetization (high-temperatures).

Various authors^[5,14] have indicated that the dis-

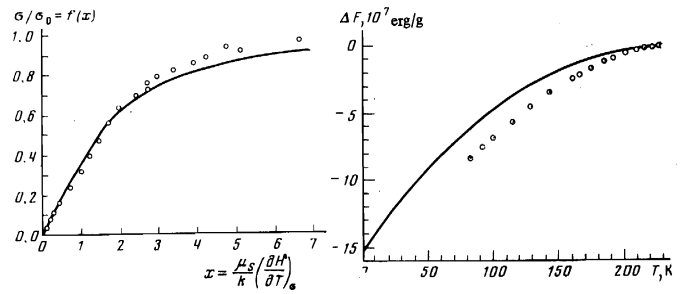


FIG. 5

FIG. 6

FIG. 5. Plot of $f(x)$ for terbium in accord with relation (2): points—experiment, solid curve—Brillouin function $B_6(x)$.

FIG. 6. Gain in the terbium free energy $\Delta F(T)$ due to the onset of ferromagnetic order: points—experiment, the solid curve was calculated from relations (4), (5), and (9).

crepancy between theory and experiment at large values of the terbium magnetization (low temperatures) can be attributed to polarization of the conduction electrons, which leads to higher experimental values of the magnetization than predicted by the molecular field theory. It can be demonstrated by the results of our measurements that the deviation of the experimental temperature dependence of the magnetization of terbium from the predictions of the molecular field theory is connected not only with the polarization of the conduction electrons, but also with the magnetoelastic contribution made to the free energy by the ferromagnetic state. The magnetoelastic deformations in terbium at nitrogen temperature reach values on the order of 10^{-2} .^[7] The magnetoelastic energy connected with these deformations is of the order of 10^7 erg/g. It is easy to show thermodynamically that the free-energy gain connected with the onset of magnetic order is described by the relation

$$\Delta F(T) = - \int_0^{T_c} \left[\int_0^{\sigma_S(T')} \left(\frac{\partial H}{\partial T} \right)_\sigma d\sigma \right] dT'. \quad (9)$$

Here $\sigma_S(T)$ is the spontaneous magnetization and T_c is the magnetic-ordering temperature.

The experimental temperature dependence of $\Delta F(T)$ of terbium, obtained by us from measurements of the magnetization with the aid of relation (9), is shown in Fig. 6. The solid curve shows the theoretical $\Delta F(T)$ calculated with the aid of relations (4), (5), and (9). The calculation was carried out at $\mu_S = 9\mu_B$, $\sigma_0 = 316$ G-cm³/g, and $T_c = 230^\circ$ K. It is seen that at nitrogen temperature the experimental $\Delta F(T)$ exceed in absolute magnitude the calculation results by 2×10^7 erg/g, i.e., by an amount of the same order as the magnetoelastic energy. This means that allowance for the magnetoelastic energy is imperative when an analysis is made of the deviations of the experimental data for terbium from the molecular-field theory.

The Callens have shown^[15] that the magnetoelastic deformations in heavy rare earths at low magnetizations are proportional to the square of the magnetization, and at high magnetization to the cube of the magnetization. The magnetoelastic energy is in turn proportional to the square of the magnetoelastic deformations. This circumstance can qualitatively explain why the experimental $\sigma_H(T)$, $H_m(\sigma)$, and $f(x)$ at low values of the magnetization agree with the molecular field theory much better than at large magnetizations (Figs. 3, 4, 5). The cause of the deviation of the experimental data from the molecular

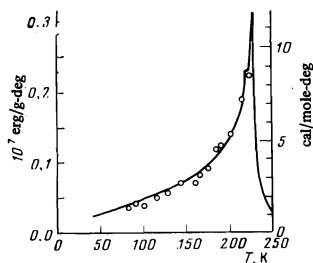


FIG. 7. Magnetic contribution to the heat capacity of terbium as obtained from measurements of the magnetization of the magnetization. Solid curve—data of [8, 9].

field theory can also be the ordering influence of the magnetic uniaxial anisotropy, the energy of which in terbium is very high and reaches $\approx 4 \times 10^7$ erg/g at nitrogen temperatures. [1] This value is comparable in order of magnitude with the free-energy gain calculated in the molecular-field approximation with the aid of relation (9), which amounts to 6×10^7 erg/g for terbium at liquid-nitrogen temperature (see Fig. 6). The uniaxial-anisotropy energy can therefore make a noticeable contribution to the effective magnetic-ordering field. The anisotropy energy depends on the magnetization in a more complicated manner than the exchange-interaction energy in the molecular-field approximation. [16] Consequently, the contribution of the anisotropy to the effective field depends on the magnetization in a different manner than the molecular field (5), and this can lead to deviations of the experimental data from the theory.

From the results of our measurements we can find the magnetic contribution to the heat capacity of terbium. It is of interest to compare it with the published data. The magnetic contribution to the heat capacity was obtained from the experimental values of $(\partial H/\partial T)_G$ and $(\partial \sigma/\partial T)_H$ for the case of a zero external field with the aid of the relation

$$C_M(T) = C_H(T) - C_G(T) = -T(\partial H/\partial T)_G(\partial \sigma/\partial T)_H. \quad (10)$$

The results are shown in Fig. 7. The solid curve is the temperature dependence of the magnetic contribution to the heat capacity in accord with the data of [8, 9]. In [8] they measured the heat capacity $C_H(T)$ in the absence of an external field. In [9] they calculated the heat capacity $C_G(T)$ of terbium at constant magnetization, on the basis

of data on inelastic neutron scattering. The solid curve of Fig. 7 is the difference $C_M(T) = C_H(T) - C_G(T)$ between the indicated functions. It is seen that our results agree well with the data of [8, 9].

The authors thank R. Z. Levitin and I. L. Aptekar' for useful discussions.

- ¹R. Z. Levitin and B. K. Ponomarev, Zh. Eksp. Teor. Fiz. **53**, 1978 (1967) [Sov. Phys.-JETP **26**, 1121 (1968)].
- ²J. J. Rhyne, S. Foner, E. J. McNiff, and R. Doclo, J. Appl. Phys. **39**, 892 (1968).
- ³K. R. Belov, R. Z. Levitin, and B. K. Ponomarev, J. Appl. Phys. **39**, 3285 (1968).
- ⁴S. Chikazumi, S. Tanuma, I. Oguro, F. Ono, and K. Tajima, IEEE Trans. Magnetics, mag-5, 265 (1969).
- ⁵D. E. Hegland, S. Legvold, and F. H. Spedding, Phys. Rev. **131**, 158 (1963).
- ⁶I. Jacobs and P. Lawrence, Rev. Sci. Instrum. **28**, 713 (1958).
- ⁷K. P. Belov, M. A. Belyanchikova, R. Z. Levitin, and S. A. Nikitin, Redkozemel'nye ferro- i antiferromagneti (Rare-Earth Ferro- and Antiferromagnets), Nauka, 1965.
- ⁸L. D. Jennings, R. M. Stanton, and F. H. Spedding, J. Chem. Phys. **27**, 909 (1957).
- ⁹J. C. G. Houmann and R. M. Niclow, Phys. Rev. **B1**, 3943 (1970).
- ¹⁰B. K. Ponomarev and S. V. Aleksandrovich, Zh. Eksp. Teor. Fiz. **67**, 1965 (1974) [Sov. Phys.-JETP **40**, 811 (1975)].
- ¹¹M. I. Darby and K. N. Taylor, Physics of Rare Earth Solids, Barnes and Noble (Russ. transl., Mir, 1974).
- ¹²D. M. Edwards and E. P. Wohlfarth, Proc. R. Soc. **A303**, 127 (1968).
- ¹³E. P. Wohlfarth, J. Appl. Phys. **39**, 1061 (1968).
- ¹⁴S. H. Liu, Phys. Rev. **139**, 470 (1961).
- ¹⁵E. Callen and H. B. Callen, Phys. Rev. **139**, A455 (1965).
- ¹⁶E. Callen and H. B. Callen, J. Phys. Chem. Solids **27**, 1271 (1966).

Translated by J. G. Adashko

148